UMYU Scientifica, Vol. 4 NO. 4, December 2025, Pp 215 – 230
https://doi.org/10.56919/usci.2544.018
ISSN: 2955 – 1145 (print); 2955 – 1153 (online)
A periodical of the Faculty of Natural and Applied Sciences, UMYU, Katsina

ORIGINAL RESEARCH ARTICLE

A Comprehensive *in Vitro* and *in Vivo* Evaluation of the Antioxidant and Antidiabetic Potential of an Okra (*Abelmoschus esculentus*) Nutraceutical Formulation

Muhammad, I[1]*; Matazu K.I[1]; Nasir, A[1]; Yau', S[1]; Suleiman, Z.A[1]; Kankia H.I[1]; Usman B[1]; Yaradua, A. I[1]; Shamsu, S[1]; Nasir, R[1]; Aminu G. B[1], Musa T[1]; Shamadeen A. K[1]; Sani, A.S[1]; Lawal, R.G[1]; Rawayau, M. A[1]; Darma, I. S[1]; Muhammad A. N[1], Matazu, H. K[2], Abbas A. Y[3]; and Bilbis, L.S[3]

[1]Department of Biochemistry, Faculty of Natural and Applied Sciences, Umaru Musa Yar'adua University, P.M.B. 2218, Katsina, Nigeria
[2]Department of Basic and Applied Sciences, College of Science and Technology, Hassan Usman Katsina Polytechnic, Katsina, Nigeria.
3Department of Biochemistry, Faculty of Science, Usmanu Danfodiyo University, P.M.B. 2346, Sokoto, Nigeria

ABSTRACT

Nutraceuticals with strong antioxidant properties offer a promising approach for managing various oxidative stress-related disorders, including diabetes. This study evaluated the antioxidant and antihyperglycaemic potentials of the previously developed okra-based antidiabetic nutraceutical formulation derived from the Ex-Maradi variety of *Abelmoschus esculentus* in alloxan-induced diabetic rats. Phytochemicals and *in vitro* antioxidant capacity of the formulation were assessed by measuring total phenolic content (TPC), total flavonoid content (TFC), and scavenging activities against DPPH, superoxide (O_2^{*-}) and hydrogen peroxide (H_2O_2). Furthermore, *in vivo* antioxidant parameters, including SOD, CAT, GPx, GSH, MDA, and essential antioxidant minerals (Zn, Cu, Mn, and Fe), were evaluated in both the serum and tissue homogenates of diabetic rats. The formulation exhibited good TPC (61.84 ± 5.31 mg GAE/g) and TFC (18.31 ± 2.17 mg QE/g) content. It also demonstrated strong free radical scavenging activities with low IC_{50} values of (0.086 ± 0.022, 0.064 ± 0.014, and 0.16 ± 0.03) mg/mL against DPPH, O_2^{*-} and H_2O_2, respectively. *In vivo*, administration of the formulation at doses of 250 and 500 mg/kg body weight for three weeks significantly ($P < 0.05$) ameliorated the elevated blood glucose levels in alloxan-induced hyperglycaemic rats, lowering them by about 56.66% at the 500 mg/kg dose. Additionally, it improved the activities of antioxidant enzymes (SOD, CAT, and GPx) and increased the concentrations of antioxidant minerals (Zn, Cu, Mn, and Fe) compared to the diabetic control group. These findings highlight the nutraceutical formulation's potent antioxidant and antihyperglycaemic properties, underscoring its potential as a therapeutic option for managing diabetes and conditions associated with oxidative stress.

ARTICLE HISTORY

Received June 13, 2025
Accepted December 04, 2025
Published December 30, 2025

KEYWORDS

Abelmoschus esculentus, nutraceutical formulation, antioxidant capacity, oxidative stress, and alloxan-induced hyperglycemic rats

INTRODUCTION

Diabetes mellitus is a metabolic disorder characterized by chronic hyperglycemia due to defects in insulin production, insulin sensitivity, or insulin availability (Dilworth et al., 2021). It manifests as Type 1 diabetes (T1D), caused by pancreatic beta-cell dysfunction, or Type 2 diabetes (T2D), resulting from insulin resistance (Tesauro & Mazzotta, 2020). Both types contribute significantly to global health challenges, with oxidative stress playing a key role in disease progression and complications affecting multiple organs (Kharroubi & Darwish, 2015). The imbalance in antioxidant defense mechanisms, including SOD, CAT, GPx, and GSH, exacerbates diabetic pathology and its complications (Sharifi-Rad et al., 2020).

Natural antioxidants, particularly plant-based nutraceuticals rich in polyphenols and flavonoids, have attracted attention for their potential to manage diabetes and oxidative stress (Roy et al., 2014). *Abelmoschus esculentus* (okra) is widely recognized for its nutritional and medicinal properties, including its hypoglycemic and antioxidant effects (Sereno et al., 2022; Tavakolizadeh et

Correspondence: Muhammad Ismaila. Department of Biochemistry, Faculty of Natural and Applied Sciences, Umaru Musa Yar'adua University, P.M.B. 2218, Katsina, Nigeria. ✉ ismaila.muhammad@umyu.edu.ng.

How to cite: Muhammad, I., Matazu, K. I., Nasir, A., Yau', S., Suleiman, Z. A., Kankia, H. I., Usman, B., Yaradua, A. I., Shamsu, S., Nasir, R., Aminu, G. B., Musa, T., Shamadeen, A. K., Sani, A. S., Lawal, R. G., Rawayau, M. A., Darma, I. S., Muhammad, A. N., Matazu, H. K., Abbas, A. Y. & Bilbis, L. S. (2025). A Comprehensive *in Vitro* and *in Vivo* Evaluation of the Antioxidant and Antidiabetic Potential of an Okra (*Abelmoschus esculentus*) Nutraceutical Formulation. *UMYU Scientifica*, 4(4), 215 – 230. https://doi.org/10.56919/usci.2544.018

al., 2023). Its bioactive compounds, such as polyphenols, polysaccharides, mucilage, and fibers, contribute to glucose regulation, lipid metabolism, and antioxidant enzyme activity (Uddin Zim et al., 2021). Studies have also demonstrated its ability to scavenge free radicals and mitigate oxidative stress in diabetes (Patwardhan & Bhatt, 2016; Phoswa & Mokgalaboni, 2023). Extensive research demonstrates that okra (Abelmoschus esculentus), including the ex-Maradi variety, possesses significant antioxidative and antidiabetic properties, making it a strong candidate for nutraceutical development (Durazzo et al., 2018; Tavakolizadeh et al., 2023; Mokgalaboni et al., 2023). Okra is rich in polyphenols, flavonoids (notably quercetin and catechin), and polysaccharides, which contribute to its robust antioxidant activity. These compounds enhance antioxidant enzyme levels (such as SOD, CAT, and GPx), reduce oxidative stress markers, and protect tissues from oxidative damage in diabetic models (Woumbo et al., 2022; Liao et al., 2019; Kwok et al., 2025). Okra extracts and mucilage have demonstrated strong free radical scavenging abilities *in vitro*, as well as the ability to inhibit lipid peroxidation and improve antioxidant status in animal studies (Woumbo et al., 2022; Liao et al., 2019).

Okra-based formulations, including those from the ex-Maradi variety, have shown the ability to lower fasting blood glucose, improve lipid profiles, and reduce HbA1c in both animal and human studies (Woumbo et al., 2022; Nasrollahi et al., 2022; Nikpayam et al., 2021; Durazzo et al., 2018; Bahari et al., 2024; Tavakolizadeh et al., 2023; Mokgalaboni et al., 2023). The antidiabetic action is attributed to several mechanisms including: Inhibition of carbohydrate-digesting enzymes (α-amylase and α-glucosidase), leading to reduced postprandial glucose spikes (Woumbo et al., 2022; Ijarotimi et al., 2023; Elkhalifa et al., 2021). Enhancement of insulin sensitivity and modulation of key metabolic pathways (e.g., PI3K/AKT, PPAR, and Nrf2) (Liao et al., 2019; Nasrollahi et al., 2022; Durazzo et al., 2018). Promotion of pancreatic islet cell regeneration and improved glycogen synthesis in the liver (Durazzo et al., 2018; Anjani et al., 2018). Reduction of chronic inflammation and improvement in lipid metabolism (Bahari et al., 2024; Tavakolizadeh et al., 2023).

The Ex-Maradi variety of *A. esculentus*, cultivated in Niger, West Africa, is particularly rich in phenolic and flavonoid compounds, thereby enhancing its antioxidant and antidiabetic properties (Muhammad et al., 2018). Studies specifically on the Ex-Maradi variety confirm that both seeds and peels contribute to antidiabetic effects, with the optimal formulation (10:90%) seed:peel ratio effectively reducing glucose adsorption and diffusion, thereby controlling postprandial blood glucose, as previously reported by Muhammad et al. (2018) and Matazu et al. (2018). These formulations also show potential for pancreatic protection and regeneration, further supporting their use in diabetes management (Durazzo et al., 2018).

Our previous research explored the effects of the seeds, peels, and whole fruit of the Ex-Maradi variety of *A. esculentus* on alloxan-induced diabetic rats (Abbas et al., 2018; Muhammad et al., 2018). Further studies formulated an okra-based antidiabetic nutraceutical by optimizing the seed and peel combinations of Ex-Maradi fruit and evaluating its antidiabetic effects (Matazu et al., 2018; Muhammad et al., 2018). While the antidiabetic effect of the formulation has been reported, a comprehensive investigation of its in vivo antioxidant defence mechanisms, particularly its impact on essential antioxidant minerals and organ-specific oxidative stress, remains unexplored. Hence, this strengthens the rationale for conducting this research to investigate whether the specific formulation from the Ex maradi variety of *Abelmoschus esculentus* has superior effects.

This study evaluates the antioxidative and antihyperglycemic potential of the developed okra-based antidiabetic nutraceutical formulation in alloxan-induced diabetic rats with oxidative stress. Using an *in-vitro* and *in-vivo* approach, its antioxidant efficacy was assessed by measuring MDA levels, antioxidant enzyme activities (SOD, CAT, GPx), and key antioxidant minerals (Zn, Cu, Mn, Fe) in the serum and organ (liver, kidney, pancreas) homogenates of the experimentally-induced oxidative stress-related diabetic rats. Additionally, its hypoglycemic effect was analyzed via an oral glucose tolerance test. Given the established role of alloxan-induced diabetes as a model for T1D in rats (Athmuri & Shiekh, 2023; Kottaisamy et al., 2021), we assess the nutraceutical's potential as a therapeutic agent for the management of oxidative stress-related diseases, including diabetes.

MATERIALS AND METHODS

2.1 Chemicals and reagents

Analytically grade laboratory chemicals and reagents were used for this study.

2.2 Formulation of the Okra-based Antidiabetic Nutraceutical

The sample of the nutraceutical formula (10:90%) seed:peel ratio, previously prepared by Muhammad et al. (2018) and evaluated by Matazu et al. (2018), was obtained from the Department of Biochemistry, Faculty of Natural and Applied Sciences, Umaru Musa Yar'adua University, Katsina State, Nigeria. The obtained sample was used throughout this research.

2.3 *In-vitro* studies

2.3.1 Preparation of extract from the nutraceutical formula

To obtain the hydro-methanolic extract from the nutraceutical formula, the extraction procedure described by Yasin et al. (2020) was followed. To do this, a precise amount (1g) of the formulation was weighed and dispersed in 100 mL of 70% methanol (1g:100 mL). The mixture was stirred and allowed to stand at room temperature (25±2^{0}C) for three (3) days with occasional stirring to extract the crude components. The entire mixture was sieved through a fine muslin cloth to obtain the filtrate (mucilage), while the solvent was allowed to evaporate at 39±2^{0}C in the drying cabinet to obtain the

mass paste concentrate of the crude extract (mucilage) labelled as 'FX', which was used for the *in-vitro* studies (Yasin et al., 2020).

2.3.2 Estimation of total phenolic content of the formulation

The total phenolic content of the nutraceutical formulation extract was determined using the Folin–Ciocalteu method as described by Phuyal et al. (2020). Briefly, 100 µL of the sample extract solution (1 mg/mL) was loaded into Eppendorf tubes in triplicate, 400 µL of distilled water was added and vortexed, then 150 µL of (10% w/v) Folin–Ciocalteu reagent (FCR) was added, spun, and allowed to react in the dark for 8 to 10 minutes. Following that, 500 µL of 20% sodium carbonate was added and vortexed. It was then incubated in a water bath at 40 °c for 20 minutes. A blank sample was also prepared by replacing the 100 µL of the extract with 100 µL of the solvent (70% Methanol) used during the process, while maintaining the same volumes of FCR and sodium carbonate as in the test sample. From each reacting mixture, 200 µL was transferred to a 96-well plate, and the absorbance was measured at 755 nm using a 96-well microplate reader. The absorbance values of the blank were subtracted from those of each corresponding sample. The same Folin-Ciocalteu assay procedure described above was applied to various concentrations (0.5, 0.25, 0.125, 0.063, 0.031, 0.016, 0.008, and 0.004 mg/mL) of the standard (gallic acid) used. All determinations were performed in triplicate. A standard curve was created by plotting gallic acid concentration against corresponding absorbance in Excel. The total phenolic content of the extract was then calculated from this curve using the linear equation (y = mx + b) for gallic acid, and the results were expressed as milligrams of gallic acid equivalents per gram of the extract (mg GAE/g extract).

2.3.3 Estimation of total flavonoid content of the formulation

The total flavonoid content of the extract was determined using a colourimetric method with Aluminium chloride, as described by Phuyal et al. (2020). Briefly, 0.5 mL of each test solution and standard solutions at various concentrations (0.5, 0.25, 0.125, 0.063, 0.031, 0.016, 0.008, and 0.004 mg/mL of Quercetin) were separately placed in designated test tubes. Each was combined with 2 mL of distilled water. Next, 0.15 mL of Sodium nitrite ($NaNO_2$, 5% w/v) was added to each tube, and the mixture was allowed to stand for 6 minutes. Following this, 0.15 mL of Aluminium trichloride ($AlCl_3$, 10% w/v) was added, and the mixture was incubated for another 6 minutes. Then, 2 mL of Sodium hydroxide (NaOH, 4% w/v) was added, and the entire mixture was diluted with distilled water to a final volume of 5 ml. The mixture was mixed thoroughly and kept at room temperature for 20 minutes to allow the colour to develop. The absorbance of the pink colour was measured at 510 nm using a microplate reader, with distilled water serving as the blank. The absorbance values from the standard (Quercetin solutions) were used to plot a standard curve. All tests were performed in triplicate. The total flavonoid content of the extract was calculated using the linear equation (y = mx + b) derived from the standard curve, and expressed as milligrams of quercetin equivalents per gram of the extract (mg QE/g extract)

2.4 *In-vitro* antioxidant activity of the formulation

Three different chemical methods, namely: DPPH, Hydrogen peroxide (H_2O_2) and Superoxide (O_2^{*-}) radical scavenging assays were employed to evaluate the *in-vitro* antioxidant activity of the extract obtained from the nutraceutical formula. A stock solution (1 mg/mL) of the crude extract in 70% methanol was prepared. This stock solution was then serially diluted using 70% methanol to provide nine different concentrations: (1.0, 0.5, 0.25, 0.125, 0.063, 0.031, 0.016, 0.008 and 0.004 mg/mL). The same procedure was applied to prepare the stock solutions of the various standard antioxidants (Ascorbic acid (vit. C), Gallic acid (GA) and Quercetin (QC)) used in conducting the respective (DPPH, H_2O_2 and O_2^{*-}) antioxidant scavenging assays.

2.4.1 Estimation of DPPH radical scavenging activity

The DPPH assay measures hydrogen-donating activity and thus provides a measure of free-radical-scavenging antioxidant activity. DPPH is a purple-coloured stable free radical; it becomes reduced to the yellow-coloured diphenyl picryl-hydrazine upon reduction by antioxidant. Briefly, in a labelled 96-well microplate, 50 µL of various dilutions of the extract or standard (ascorbic acid (Vit. C) were separately mixed with 50 µL of DPPH in methanol solution (0.004%). After an incubation period of 30 min in the dark at room temperature, the absorbance of the colour change was measured at 517 nm (Apak et al., 2022). The lower the absorbance, the higher the free radical-scavenging activity. The ability to scavenge the DPPH radical was calculated by using the following equation:

$$\% \text{ Scavenging effect} = \frac{(\text{Ac} - \text{Ae})}{\text{Ac}} \times 100$$

Where Ac: control absorbance and Ae: absorbance in the presence of extract or standard.

The IC_{50} values (concentration of extract or standard necessary to decrease the initial concentration of DPPH by 50 %) were calculated and obtained by reference from the non-linear regression analysis:

$y = a\ lin(x) + b$

$50 = a\ lin\ (IC_{50}) + b$

$IC_{50} = e^{(50-b)/a}$

2.4.2 Estimation of H_2O_2 Decomposition activity

The hydrogen peroxide (H_2O_2) decomposition activity of the extract obtained from the formulation was conducted as described by Apak et al. (2022). In this method, when a scavenger is incubated with hydrogen peroxide, the decay or loss of hydrogen peroxide can be measured spectrophotometrically at 230 nm. Briefly, 2 mL of hydrogen peroxide (20 mM) in phosphate-buffered saline

was added to 1 mL of various concentrations of extract or standard (Gallic acid) in methanol. The decomposition activity was allowed to continue for 10 minutes. After 10 min, the absorbance was measured at 230 nm. The ability of the formulation to decompose the H_2O_2 was calculated by using the following equation:

$$\% \text{ Decomposition effect} = \frac{(Ac - Ae)}{Ac} \times 100$$

Where Ac: control absorbance and Ae: absorbance in the presence of extract or standard.

The IC_{50} values (concentration of extract or standard required to decrease the initial H_2O_2 concentration by 50%) were calculated from the non-linear regression analysis described in the DPPH assay above.

$y = a\ lin(x) + b$

$50 = a\ lin(IC_{50}) + b$

$IC_{50} = e^{(50-b)/a}$

2.4.3 Estimation of Superoxide Radical Scavenging Activity

The superoxide radical scavenging activity of the formulation was determined by the NBT reduction method using alkaline DMSO (Apak et al., 2022). In this method, superoxide radicals in alkaline DMSO were generated by the addition of 0.2 mL of 1% NaOH to 19.8 mL of air-saturated DMSO. The solution was allowed to stand at room temperature for 30 minutes. The generated superoxide remains stable in solution and can reduce nitro-blue tetrazolium (NBT) to the formazan dye at room temperature, which can be measured at 560 nm. Briefly, 0.1 mL of NBT (1 mg/mL in DMSO) was added to the reaction mixtures containing 1 mL of the prepared alkaline DMSO and 0.3 mL of the extract or standard at the respective concentrations (Quercetin). The absorbance was measured at 560 nm against an appropriate blank (Pure DMSO) to determine the quantity of formazan generated. Quercetin was used as a positive control. All tests were performed in triplicate. Results were expressed as percentage scavenging of superoxide ions according to the equation below:

$$\% \text{ scavenging effect} = \frac{(\text{Abs of Control} - \text{Abs of STD or Sample})}{\text{Abs of control}} \text{ x } 100$$

Where Abs of Control is the absorbance without plant extract or standard.

The IC_{50} values (concentration of extract or standard required to decrease the initial concentration of superoxide radical by 50%) were calculated from the non-linear regression analysis, as described in the DPPH assay above.

2.5 In vivo studies

2.5.1 Animals and ethics statement

This research protocol was approved by the Usmanu Danfodiyo University Sokoto's Research and Ethics Committee with approval number UDUS/UREC/2021/020. The study was carried out in 25 young male Wistar albino rats of about six to seven weeks old, weighing approximately 220–250 g. The rats were procured from Usmanu Dan Fodiyo University, Sokoto. They were placed in standard cages and housed under standard conditions in the animal house, maintaining an average ambient temperature of 22–25°C and humidity of 75%, with a 12-hour photoperiod (Hamisu and Salisu, 2025; Salisu et al., 2019, 2020; Usman et al., 2025). All animals received standard rodent chow pellets and water *ad libitum* during the experiment. The protocol for the handling and care of animals, as recommended by the ethical committee and stipulated in the guidelines for the use and care of animals, was carefully followed, with all possible efforts made to minimize animal suffering and reduce the number of rats used per experimental group.

2.5.2 Induction of diabetes and grouping of the experimental animals

The rats were randomly divided into five groups of five each. Group 1: (Normal Control [NC]), Group 2: (Diabetic Control [DC]), Group 3: (Drug control [MC]), Group 4 and Group 5: are the Formulation groups (FX_{250} and FX_{500}), respectively (Figure 1). All the rats were allowed to acclimatize for one week before the treatments. In Exception of the normal control group, diabetes was induced in all the remaining rats by intraperitoneal injection of alloxanmonohydrate at a dose of 120 mg/kg body weight as previously reported by Muhammad et al. (2018). Alloxan (98% purity, Merck) was dissolved in saline solution for the intraperitoneal (IP) injection. It was injected into the rats after 12 hours of fasting. After 6 hours of alloxan administration, the rats were allowed to drink 10 % glucose solution *ad libitum* for the next 24 hours to prevent alloxan-induced hypoglycaemia (Muhammad et al., 2018). The animals were observed for polydipsia, polyuria, and polyphagia as well as a general reduction of body weight. 72 hours after alloxan administration, the animals were fasted overnight for 12 hours, and diabetes was confirmed by measuring fasting blood glucose levels from tail vein blood samples collected with a small cut using a lancet. A glucometer and test strips were used for this estimation. Only the rats with fasting blood glucose levels greater than 7.0 mmol/L (126 mg/dL) were considered to have confirmed diabetes and included in the study (Muhammad et al., 2018; Uddin et al., 2021). For the normal control group, 2 mL/kg body weight of vehicle saline (0.9% NaCl) was administered to the rats via the same route (IP) to balance the stress of

intraperitoneal injection with that of the alloxan groups (Figure 1).

2.5.3 Experimental design and treatment of the rats

The normal group and the diabetic control group received normal saline (0.9% NaCl) orally at a dose of 2 mL/kg body weight orally once per day for three weeks. The drug control group received Metformin at a dose of 100 mg/kg body weight, while the test groups (FX_{250} and FX_{500}) received oral administration of the okra-based antidiabetic nutraceutical formulation at 250 and 500 mg/kg body weight, respectively. All treatments started after the confirmation of the induction of diabetes. Treatments were continued daily for three weeks. Fasting blood glucose levels in all groups were checked using tail vein blood samples at the end of each week throughout the experimental period, in addition to body weight changes. At the end of week three of the treatment procedures, an oral glucose tolerance test was conducted in all the rats after fasting for 12 hours. The following day, the rats were anaesthetized then sacrificed. Blood and organ samples were collected for various biochemical analyses.

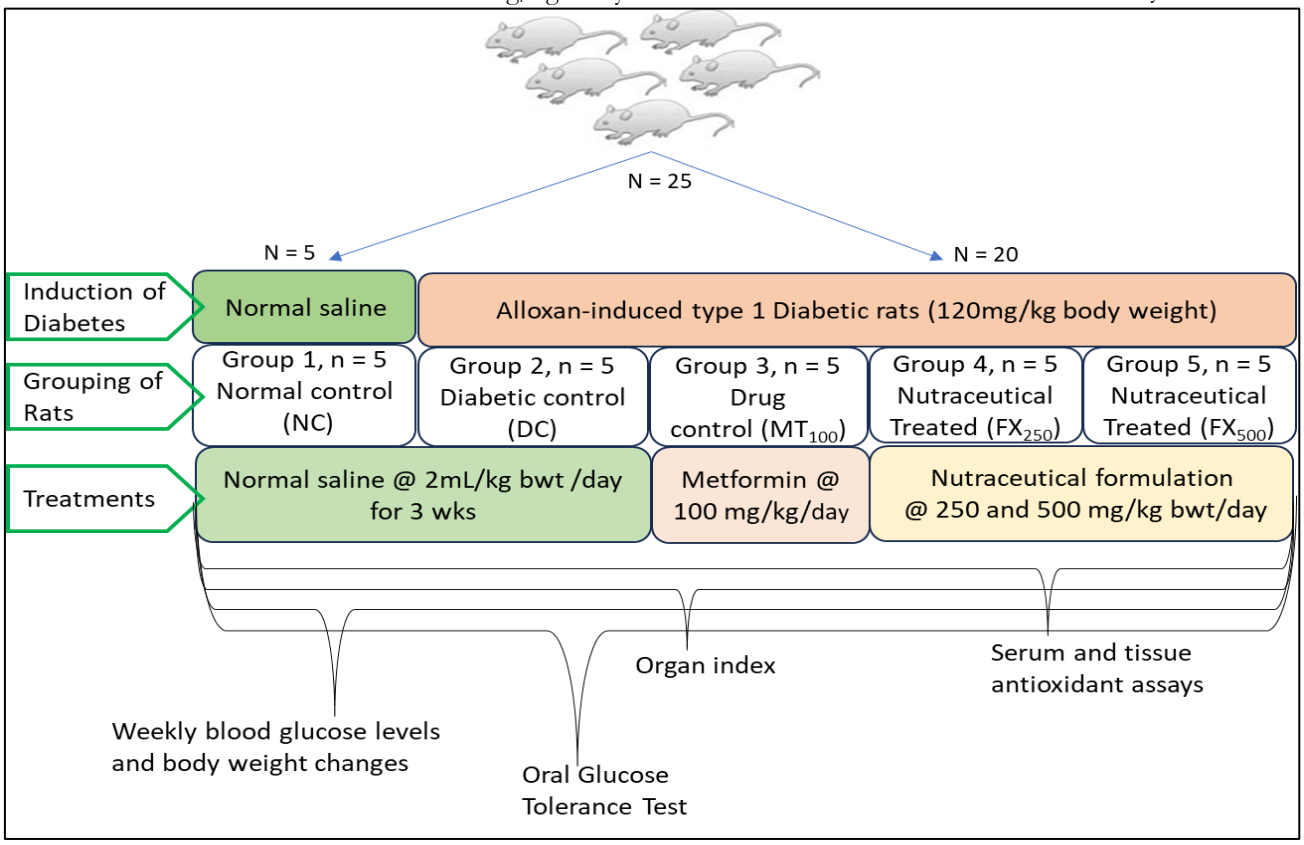

Figure 1: Experimental design: Illustrating the induction of diabetes, grouping and treatments of the experimental rats.

2.5.4 Estimation of blood glucose levels

At the end of every week of the experiment, all rats were fasted overnight for 12 hours. With the aid of a fine test glucometer and test strips, the fasting blood glucose levels were estimated directly from the blood sample obtained through the rats' tail vein puncture.

2.5.5 Oral glucose tolerance test

The oral glucose tolerance test was conducted following the protocol described by Islam et al. (2022). Briefly, after the final treatment at the end of week 3 (day 21st) of the experimental procedure, the rats were fasted overnight for 12 hours. The following morning, the fasting blood glucose levels of all the rats was measured and recorded as the baseline. Following this, a glucose-D solution (200 mg/mL) was prepared in normal saline and orally administered to all the rats at a calculated dose of 2 g/kg body weight. Subsequently, with the aid of a glucometer, the blood glucose levels of the rats were measured from blood samples collected from the rats' tail vein at 30-minute intervals for a total period of 2 hours. During the OGTT experiment, the rats were provided with *ad libitum* access to drinking water while their diet was withheld. After the experiment, the rats' diet was supplied and allowed *ad libitum*. The animals were also allowed to sit until the next day before they were sacrificed. A graph of the glucose tolerance curve was plotted using blood glucose levels on the (y-axis) against time on the (x-axis). Then, the blood glucose-lowering effect of the formulation was determined at 30-minute intervals for 120 minutes during glucose loading, assessing the rate of glucose metabolism in the respective animal groups (Islam et al., 2022).

2.5.6 Blood and organ sample collection and their preparation

At the end of the final experimental procedures, all animals were anaesthetized by intraperitoneal injection of 2.5 mL/kg body weight of Ketamine/Xylazine cocktail

solution [(Ketamine 75 mg/kg) / (Xylazine 8mg /kg)] (Yusof, 2020). Blood samples were collected through cardiac puncture and then transferred into plain tubes. The blood samples were allowed to coagulate by standing at room temperature for 30 min, then centrifuged at 1000 × g for 10 min to obtain the serum. The serum was collected in cryovials and stored in the fridge at - 4 °C until later use.

2.5.7 Isolation of organs, and estimation of organ index

After the blood sample collection, the rats were euthanized using CO_2 before the stomach was cut open. Vital organs, including the liver, kidney and pancreas were isolated, weighted and recorded to estimate the organ index based on the ratios of the organ to the live body weight of the rat as described by Sun (2022) using the formula below:

$$\text{Organ index} = \frac{\text{Organ weight (g)}}{\text{Rat live weight (g)}} \text{X } 100$$

A portion of each organ sample, according to the respective group, was cut and placed in a labelled container before being taken for homogenization. To obtain a 10 % tissue homogenate of each respective organ, 2 g of the tissue sample from respective organ was cut and rinsed with pre-chilled 0.9% saline to remove excess blood; then, carefully homogenized in 18 mL of pre-chilled 0.9% saline using mortar and pestle tissue grinder under ice. Subsequently, the mixture was centrifuged at 4,500 rpm, maintaining a temperature of 4 °C for 15 minutes. The supernatant from the tissue homogenate was used for total protein estimation and further biochemical analysis (Gunas et al., 2023).

The total protein content of the tissue homogenate was estimated using the Bradford method (Gunas et al., 2023).

2.6 In-vivo antioxidant assays

2.6.1 Estimation of lipid peroxidation product (Malondialdehyde)

The determination of lipid peroxidation in the rat's serum and tissue homogenates was conducted by estimating the concentration of Malondialdehyde (MDA) using the thiobarbituric acid reacting substances (TBARS) assay method as described by Ohkawa et al. (1979). The principle of the assay is based on the spectrophotometric measurement of the pink-coloured MDA-TBA adduct generated by the reaction of thiobarbituric acid (TBA) with MDA (a marker of oxidative stress) present in the sample. This reaction occurs under acidic and high-temperature conditions. Briefly, in labelled Eppendorf tubes, 200 µL of the serum or tissue homogenate was added to 1 mL of 10 % Trichloroacetic acid (TCA) to precipitate the proteins, then 1 mL of the TBA solution (0.67% of TBA (w/v) in 10% TCA) was added. The reaction mixtures were heated for 30 minutes in a hot water bath at 95 °C to allow the reaction between MDA and TBA to form a pink-coloured complex (MDA-TBA adducts). The reaction mixture was allowed to cool in a cold water bath, and then 2 mL of 15% TCA was added to precipitate out the proteins and other interfering substances. The mixture was centrifuged at 3,000 g for 10 minutes to separate the precipitate, leaving a clear supernatant for analysis. Then, 0.5 mL of n-butanol was added to the mixture in order to extract the developed chromophore. The mixture was centrifuged again to separate the phases.

Subsequently, the absorbance of the chromophore developed was measured at 532 nm using a spectrophotometer. A blank tube containing only reagents (no sample) was used to zero the spectrophotometer. The measured absorbance is proportional to the concentration of MDA in the sample. To quantify the MDA levels in the samples, MDA standard solution (Stock: 1 mM tetraethoxypropane in ethanol) was used. Tetraethoxypropane hydrolyses to MDA and serves as the standard. A calibration curve was made using the MDA standard solutions (0.04, 0.08, 0.16, 0.32, 0.64, 1.28, and 2.56) µM. The absorbance values of the MDA standards were plotted against their known concentrations.

$$\text{MDA concentration} = \frac{\text{Absorbance of sample}}{\text{Slope of calibration curve}}$$

The final results for MDA concentrations were expressed as µM/mL for serum samples and µM/mg protein for tissue homogenate samples (Ohkawa et al., 1979).

2.6.2 Determination of reduced glutathione (GSH) concentration

The levels of reduced glutathione (GSH) were determined using the Ellman's reagent (5,5'-dithiobis-(2-nitrobenzoic acid (DTNB)) solution as described by Ellman (1961). This method is based on the reaction of DTNB with the sulfhydryl (-SH) group of GSH to form a yellow-coloured product called TNB (5-thio-2-nitrobenzoic acid) that can be measured spectrophotometrically. Briefly, the serum or tissue homogenate was deproteinized by using metaphosphoric acid (MPA) to remove interfering proteins. To do this, 0.1 mL of serum or tissue homogenate sample was mixed with 1.9 mL of 5% metaphosphoric acid (MPA), then centrifuged at 10,000 × g for 10 minutes to obtain the clear supernatant. 100 µL of the deproteinized serum or tissue supernatant was mixed with 100 µL of 5 mM (0.05) DTNB solution (freshly prepared in phosphate buffer, PH 7.4). Then, 800 µL of 0.1 M Phosphate buffer (PH 7.4) was added and mixed. For the GSH standards, concentrations (10, 20, 40, 60, 80, and 100 µM) of GSH were prepared and mixed using the same proportions as the sample (100 µL standard + 100 µL DTNB + 800 µL buffer). The reaction mixture was incubated at room temperature for 10 minutes to allow the reaction and colour development to occur. The intensity of the yellow colour product developed in the reaction is directly proportional to the concentration of reduced glutathione in the sample. The absorbance of the sample was measured at 412 nm using a spectrophotometer. A blank reaction mixture (phosphate buffer + DTNB without GSH) was used to

zero the instrument. The concentration of reduced glutathione in the samples was determined from absorbance values using a standard curve prepared with known concentrations of GSH. The GSH concentration in the sample was calculated using the equation from the calibration curve:

$$\text{GSH concentration} = \frac{\text{Absorbance of sample}}{\text{Slope of calibration curve}} \times \text{Dilution factor}$$

The results are expressed as µM/mL of GSH for serum and µM/mg of protein for tissue homogenates.

2.6.3 Estimation of catalase (CAT) activity

Quantification of catalase activity was performed according to the method of Aebi (1984). This method relies on catalase's ability to catalyze the breakdown of H_2O_2 into water and oxygen. The decrease in H_2O_2 concentration, which has strong absorbance at 240 nm is monitored spectrophotometrically. A reduction in absorbance over time is proportional to the catalase activity in the sample. Briefly, 250 µL of 50 mM PBS, pH 7, was added to a labelled 96-well microplate, and then 15 µL of the sample (serum or tissue homogenate) was added. It was mixed, and the absorbance was read at 240 nm to obtain the blank reading (A_0). With the aid of a multichannel pipette, 5 µL of 6% H_2O_2 in PBS pH 7 was immediately added to each well, and the mixture was mixed by pipetting to initiate the reaction. After a minute (60 seconds) of reaction, the mixture was read again at 240 nm to obtain the post-reaction absorbance (A_1). The average change in hydrogen peroxide absorbance per minute was calculated using the following formula:

$$\text{Catalase activity} = \frac{\Delta A \cdot V\,\text{total}}{\varepsilon \cdot d \cdot Vsample}$$

Catalase activity was expressed in IU $mL^{-1}min^{-1}$ for serum and IU mg $protein^{-1}min^{-1}$ for tissue homogenates.

Where:

ΔA: Change in absorbance per minute (A_0 - A_1).

V_{total}: Total reaction volume in the well (0.270 mL).

ε: Extinction coefficient of H_2O_2 at 240 nm (0.0436 mM^{-1} cm^{-1}).

d: Path length (0.6 cm in a 96-well microplate).

V_{sample}: Volume of the sample added (0.015 mL).

2.6.4 Estimation of superoxide dismutase (SOD) activity

Superoxide dismutase (SOD) activity was quantified according to the method described by Marklund and Marklund (1974). The principle of this procedure is based on the ability of SOD to inhibit the generation of superoxide anion radicals (O_2^-) during the auto-oxidation of pyrogallol in an alkaline environment. SOD catalyzes the dismutation of O_2^- into oxygen (O_2) and hydrogen peroxide (H_2O_2). The assay quantifies the extent of SOD inhibition of pyrogallol auto-oxidation by measuring the reduction in absorbance at 325 nm. Briefly, in a labelled 96-well microplate, 200 µL of 50 mM Tris-HCl buffer containing 1 mM EDTA at pH 8.2 was mixed with 50 µL of the sample (serum or tissue supernatant), alongside a blank of distilled water. The mixtures were thoroughly mixed by pipetting. Then, the initial absorbance was measured at 325nm using a microplate reader and recorded. The reaction was initiated by adding 50 µL of 24 mM pyrogallol solution to the wells, then mixing thoroughly by pipetting. The absorbance was measured again at 325 nm over 60 seconds, with readings taken at 15-second intervals. The rate of pyrogallol auto-oxidation in the presence of the sample decreases relative to the blank. One unit (U) of SOD activity is defined as the amount of enzyme required to inhibit pyrogallol auto-oxidation by 50%. The SOD activity was determined by comparing the auto-oxidation rate of pyrogallol (change in absorbance per minute) in the presence and absence of the sample, using the formula below:

$$\text{SOD activity} = \frac{\text{Rate in Blank} - \text{Rate in sample}}{\text{Ratein Blank}} \times 50$$

Where:

Rate in Blank: Change in absorbance per minute in the absence of the sample.

Rate in Sample: Change in absorbance per minute in the presence of the sample.

50% inhibition: Defined as 1 unit (U) of SOD activity.

2.6.5 Estimation of Glutathione peroxidase (GPx) activity

Glutathione peroxidase (GPx) activity was estimated using the indirect assay method described by Lawrence and Burk (1976). The principle involves measuring the enzyme's (GPx) ability to catalyze the reduction of hydrogen peroxide (H_2O_2) to H_2O and O_2 using reduced glutathione (GSH) as a substrate. Oxidized glutathione (GSSG) is recycled back to GSH by glutathione reductase (GR) in the presence of NADPH. The decrease in NADPH absorbance at 340 nm, proportional to GPx activity in the sample, is monitored spectrophotometrically. Briefly, in labelled Eppendorf tubes, the reaction mixture containing 0.5 mL of 50 mM PBS (at pH7.0), 0.1 mL of 1 mM EDTA solution, 0.1 mL of 2 mM GSH solution, 0.05 mL of 0.2 mM NADPH solution, 0.05 mL of 0.24 U/mL of GR and 0.1 mL of sample (serum or tissue homogenate) were mixed thoroughly by pipetting. Then, 200 µL of the mixture was placed in a 96-well microplate, and the initial absorbance (A1) was measured at 340 nm using a microplate reader. To simulate the reaction, 25 µL of 1.5 mM H_2O_2 was added and mixed thoroughly. Subsequently, the change in absorbance (A2) was measured again at 340 nm for a period of 3 minutes at 30-second intervals. GPx activity

(U/mL or U/mg protein) was calculated using the following formula below:

Firstly, the rate (ΔA) of NADPH consumption was calculated:

$$\text{Rate of NADPH consumption } (\Delta A) = \frac{A1 - A2}{\text{Time in minutes}}$$

Then, the GPx activity can be calculated using the molar extinction coefficient (ε) of NADPH at 340 nm as follows:

$$\text{GPx activity} = \frac{\Delta A}{\varepsilon \times \text{reaction volume (mL)}}$$

The amount of enzyme that catalyzes the conversion of 1 µmol of NADPH per minute.

2.6.6 Estimation of antioxidant mineral concentrations

For the trace element analysis, atomic absorption spectroscopy (AAS) was used to quantify the selected trace elements, including Zinc (Zn), Copper (Cu), Manganese (Mn), and Iron (Fe), as outlined by Kizalaite (2019). This procedure involves sample digestion, preparation of standards, calibration of the instrument, and element detection. The principle is based on the release of elements from the sample into the solution via microwave digestion with concentrated acids. Then the elements are quantified by AAS, where their (elements) specific absorption at characteristic wavelengths is measured. Briefly, plasma and the various organ homogenate samples were prepared by microwave digestion as described by Kizalaite (2019) as follows: 0.5 mL of each sample was deposited into labelled microwave digestion vessels. To each vessel, 5 mL of concentrated nitric acid (70% HNO_3) and 1 mL of hydrogen peroxide (30% H_2O_2) were added, covered with the vessel lid, and then submitted to the microwave at 200˚C for 20 minutes. After digestion and cooling, the samples were transferred into 25 mL volumetric flasks, diluted to the mark with deionized water, then filtered to remove any particulate matter. Subsequently, the samples were further analyzed using an atomic absorption spectrometer equipped with a deuterium background corrector, while hollow cathode lamps for Zn, Cu, Mn, and Fe were used as radiation sources. Atomization was carried out in an air-acetylene flame. The operational conditions were established according to the manufacturer's recommendations for each element. The results are presented in µg/mL for plasma and µg/g wet tissue for the organ samples.

2.7.0 Data Analysis

The data obtained were presented as mean ± standard error of the mean (SEM). Data from 3 sample replicates (n=3) per treatment in each group were used for statistical analysis across groups. Results for the biochemical parameters were analyzed statistically using one-way analysis of variance (ANOVA) followed by Duncan's post hoc multiple-comparison tests in SPSS version 20. A p-values ≤ 0.05 were considered statistically significant.

RESULTS

3.1.0 *In-vitro* studies

3.1.1 Total phenolic content, total flavonoid content, and the in-vitro antioxidant activity of the formulation

The results for the estimations of total phenolic content, total flavonoid contents and the *in-vitro* antioxidant activity of the nutraceutical formulation (FX) are presented in Figure 2. The results showed that the formulation exhibited a good concentration of phenolic and flavonoid compounds, with estimated TPC and TFC values of 61.84±5.31 mgGAE/g and 18.31±2.17 mgQE/g, respectively (Figure 2A). This indicated that the nutraceutical formulation is rich in phenolic compounds, which are known to contribute to its antioxidant potential.

The free radical scavenging activities of the FX extract were evaluated against DPPH, superoxide ($O_2^{\bullet-}$), and hydrogen peroxide (H_2O_2), with the results presented in Figures 2B, 2C, and 2D, respectively. The formulation demonstrated dose-dependent radical scavenging activity with IC_{50} values of 0.086 ± 0.022 mg/mL for DPPH; 0.064 ± 0.014 mg/mL for $O_2^{\bullet-}$; and 0.16 ± 0.03 mg/mL for H_2O_2 as compared to the IC_{50} values of the standard antioxidants used (0.031 ± 0.001 mg/mL for vitamin C; 0.024 ± 0.002 mg/mL for quercetin; and 0.063 ± 0.01 mg/mL for gallic acid). The FX extract exhibited relatively strong, but lower, radical-scavenging activity. These findings suggest that while the formulation possesses significant antioxidant potential, its efficacy is slightly lower than that of pure standard antioxidants (vitamin C; quercetin and gallic acid). Nonetheless, the results confirm that the nutraceutical formulation has notable free radical scavenging activity, supporting its potential therapeutic application in oxidative stress-related conditions.

3.2.0 *In-vivo* studies

3.2.1 Induction of diabetes and effect of FX administration on blood glucose levels

Intraperitoneal administration of a single dose (120 mg/kg body weight) of alloxan to 12-hour fasted rats resulted in a significant ($P < 0.05$) elevation of fasting blood glucose levels reaching 16.48 mmol/L, compared to the normal control rats with a blood glucose level of 5.72 mmol/L. This hyperglycemic state was observed after three days of alloxan administration. Additionally, clinical symptoms of diabetes, including polydipsia, polyphagia, polyuria, and general stress conditions, were observed in the diabetic rats.

The fasting blood glucose levels monitored weekly throughout the study are presented in Figure 3A. The results indicate that alloxan administration led to a persistent and significant ($P < 0.05$) elevation in fasting blood glucose levels, peaking at 19.48 mmol/L at week three (3) in the diabetic untreated rats, whereas the normal control group maintained a fasting blood glucose level of

5.72 mmol/L (Figure 3A). However, administration of the nutraceutical formulation (FX) at 250 mg/kg and 500 mg/kg body weight significantly ($P < 0.05$) reduced blood glucose levels compared with diabetic untreated rats (Figure 3A). The steady weekly reduction in blood glucose levels in the FX_{250} and FX_{500}-treated groups indicated gradual normalization, approaching those of the normal control and metformin-treated groups by the third week (Figure 3A). In addition, at week three, there was no significant ($P > 0.05$) difference in blood glucose levels between the metformin-treated group (MC_{100}) and the FX_{500}-treated group (Figure 3A).

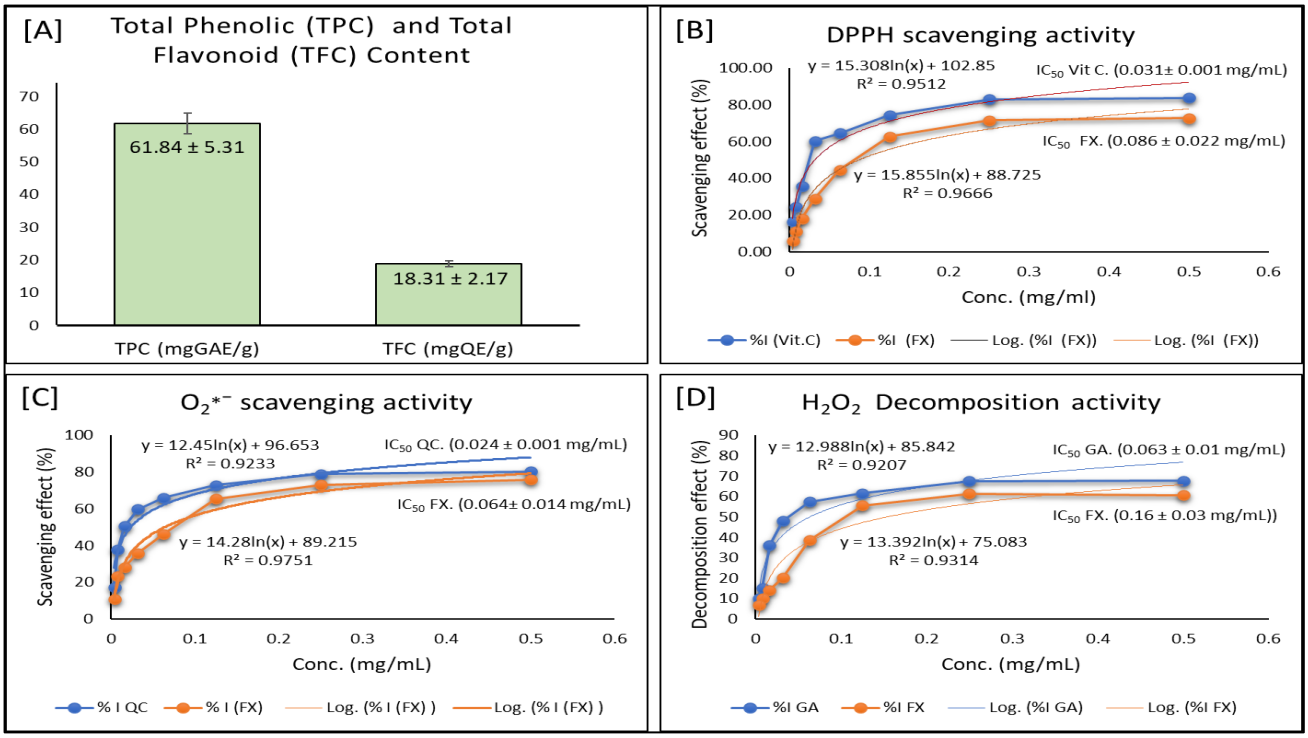

Figure 2: Phytochemicals and *in-vitro* antioxidant activities of 'FX' formulation.[A]: Total phenolic andtotal flavonoid content;[B]: DPPH radical scavenging activity;[C]: O_2^{*-} radical scavenging activity and [D]: H_2O_2 decomposition activity. Values are presented as mean ± SEM(n = 3).

3.2.2 Effect of FX administration on Body weight changes

The results of the effect of FX administration on body weight changes are presented in Figure 3B. Administration of alloxan resulted in a significant ($P < 0.05$) decrease in body weight in diabetic rats, evident from week 1 through week 3 (Figure 3B). While no significant ($P > 0.05$) weight changes were observed in any group at baseline (week 0), the normal control group showed a steady, significant ($P < 0.05$) increase in body weight throughout the experimental period. The diabetic control (DC) group exhibited a progressive reduction in body weight, decreasing from 231.41 g at week 0 to 185.26 g at week 3, whereas the normal control group increased from 232.10 g at week 0 to 265.13 g at week 3. Treatment with FX_{250} and FX_{500} resulted in a gradual and significant ($P < 0.05$) increase in body weight compared with untreated diabetic rats (Figure 3B). This suggests that FX administration contributed to weight maintenance and mitigated the weight loss associated with alloxan-induced diabetes.

3.2.3 Effect of FX administration on oral glucose tolerance test

The results of the oral glucose tolerance test are depicted in Figure 3C. The basal fasting blood glucose level was significantly higher in the diabetic control group than in the other groups. Following the oral glucose load, a sharp increase in blood glucose levels was observed in all groups within the first 30 minutes, with the diabetic control group reaching a peak value of 21.05 mmol/L (Figure 3C). Subsequently, blood glucose levels began to decline steadily after 60 minutes and returned to near-normal levels at 90 and 120 minutes in all groups except the diabetic control, which exhibited delayed glucose clearance, as evidenced by a slight decline at 90 minutes followed by a plateau up to 120 minutes. This result indicates impaired glucose metabolism in the diabetic control rats (Figure 3C).

3.2.4 Effect of FX administration on organ index

The results of the organ index analysis are presented in Figure 3D. A slight decrease in liver index was observed in all diabetic rat groups (DC, MC, FX_{250}, and FX_{500}) compared to the normal control (NC) group. However, there were no significant ($P > 0.05$) differences in liver indices between all the treated rats (NC, MC, FX_{250}, and FX_{500}) (Figure 3D). Also, no significant differences ($P > 0.05$) in kidney indices were observed among the experimental groups (NC, DC, MC, FX_{250}, and FX_{500}), including the diabetic control group. Regarding pancreatic indices, the diabetic control group showed a significantly lower pancreatic index (0.12 mg/g; $P < 0.05$) than the

normal control group (0.24 mg/g; Figure 3D). However, administration of FX_{250} and FX_{500} significantly ($P < 0.05$) increased the pancreatic index, restoring it to levels comparable to those of the normal control group. Additionally, there were no significant differences ($P > 0.05$) in the pancreatic index among the FX_{250}, FX_{500}, MC_{100}, and normal control (NC) groups (Figure 3D).

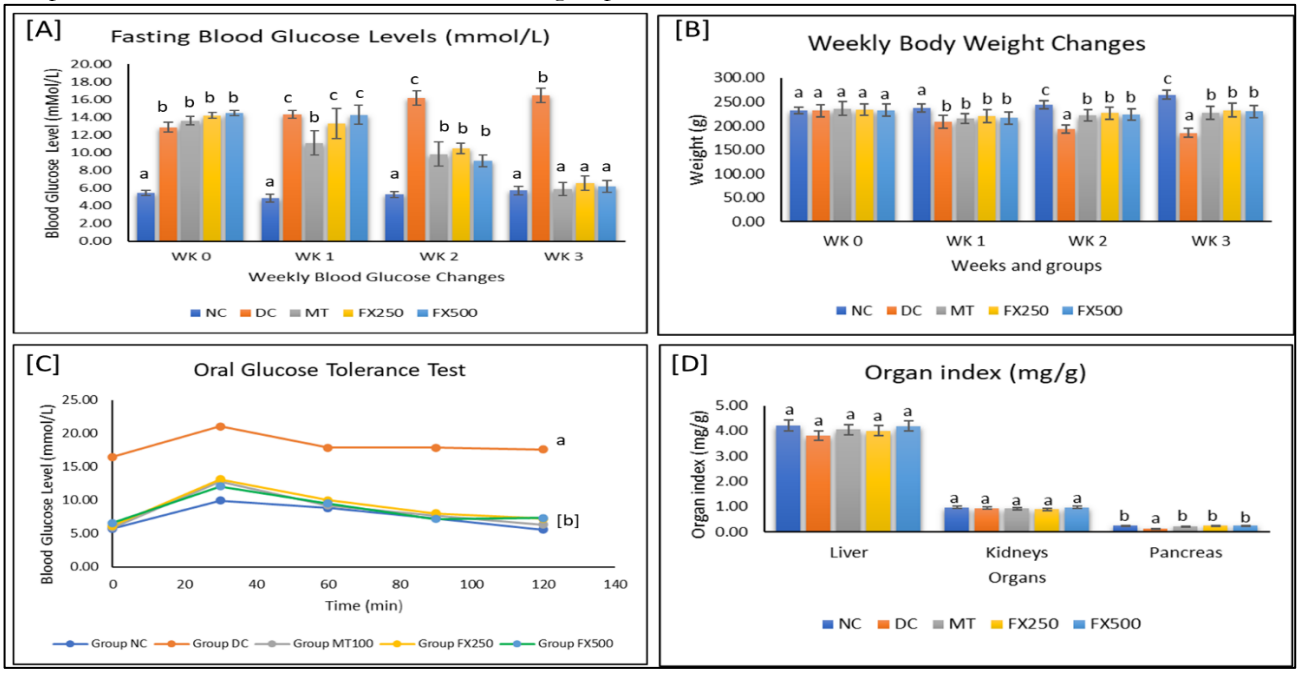

Figure 3: Effect of FX administration on blood glucose level, body weight changes and organ indices.[A]: Fasting lood glucose levels, [B]: Weekly body weight changes, [C]: Oral glucose tolerance test and [D]: Organ indices. Values are presented as mean ± SEM;n= 3. The experimental groups are: NC (Normal Control), DC (Diabetic Control), MC (Metformin-treated group), and FX_{250} and FX_{500} (formulation-treated groups). Superscript letter ('a' 'b') indicates statistically significant differences between groups at $P \leq 0.05$ level of significance.

Table 1A: Serum antioxidant enzyme activities

Group	MDA (nmol/mL)	GSH (µmol/L)	CAT (U/mL)	SOD (U/mL)	GPx (U/mL)
NC	1.61 ± 0.33^{a}	4.99 ± 0.54^{b}	317.11 ± 38.19^{b}	136.16 ± 7.45^{b}	143.71 ± 4.79^{b}
DC	5.77 ± 0.87^{b}	0.66 ± 0.06^{a}	150.27 ± 13.47^{a}	60.85 ± 11.02^{a}	85.58 ± 8.52^{a}
MT	1.63 ± 0.21^{b}	5.66 ± 0.92^{c}	250.40 ± 31.53^{b}	135.07 ± 7.24^{b}	136.27 ± 12.44^{b}
Fx250	1.97 ± 0.77^{b}	3.47 ± 0.62^{b}	293.95 ± 7.04^{b}	136.24 ± 7.93^{b}	136.97 ± 6.49^{b}
Fx500	2.01 ± 0.11^{b}	4.68 ± 0.45^{c}	305.38 ± 15.42^{b}	139.33 ± 4.7^{b}	139.25 ± 7.5^{b}

Table 1B: Liver antioxidant enzymes activities

Grp	MDA (nmol/mg Prot)	GSH (µmole/g Prot)	CAT (U/mg Prot)	SOD (U/mg Prot)	GPx (U/mg Prot)
NC	1.04±0.08^{a}	5.32± 1.01^{b}	660.27 ± 80.71^{c}	569.49± 155.34^{a}	277.04± 53.44^{a}
DC	4.11 ±0.49^{b}	4.16±0.79^{a}	350.40 ± 76.76^{a}	727.51± 47.31^{a}	518.68± 61.09^{a}
MT	1.56±0.45^{a}	5.43±0.39^{b}	493.95 ± 7.04^{b}	568.4± 52.96^{a}	236.27± 12.44^{a}
Fx250	1.30 ±0.43^{a}	3.87±0.64^{a}	517.11 ± 38.19^{b}	636.31± 92.57^{a}	228.97± 5.82^{a}
Fx500	1.61 ± 0.29^{a}	5.01 ± 0.82^{b}	575.38 ± 39.02^{b}	605.96 ± 15.14^{a}	252.56 ± 30.16^{b}

Table 1C: Kidney antioxidant enzymes activities

Grp	MDA (nmol/mg Prot)	GSH (µmol/g Prot)	CAT (U/mg Prot)	SOD (U/mg Prot)	GPx (U/mg Prot)
NC	0.96±0.15^{a}	5.65±0.06^{c}	432.11± 68.82^{b}	492.09± 48.91^{a}	210.29 ± 53.81^{b}
DC	2.77±0.98^{b}	1.19±0.35^{a}	269.97± 16.26^{a}	233.38± 30.97^{b}	91.95± 3.39^{a}
MT	1.23± 20^{a}	4.93 ± 0.70^{bc}	423.77± 94.88^{b}	481.87± 43.39^{a}	186.57± 41.84^{b}
Fx250	1.30±0.43^{a}	4.37±0.58^{b}	403.39± 17.48^{b}	529.81± 58.33^{a}	162.3± 58.84^{ab}
Fx500	1.17±0.13^{a}	5.34±0.40^{bc}	470.75± 70.18^{b}	545.86± 16.04^{a}	208.96± 49.15^{b}

Table 1D: Pancreas antioxidant enzymes activities

Grp	MDA(nmol/mg Prot)	GSH (µmol/g Prot)	CAT (U/mg Prot)	SOD (U/mg Prot)	GPx (U/mg Prot)
NC	0.84±0.08^{b}	5.26±0.41^{b}	517.11± 38.19^{c}	569.49± 155.34^{b}	317.04± 60.88^{c}
DC	4.71±0.64^{a}	0.63±0.20^{a}	193.60± 39.38^{b}	194.18± 50.24^{a}	152.01± 46.33^{c}
MT	0.97±0.19^{b}	4.30 ±0.61^{b}	383.79 ± 26.61^{b}	568.40 ± 52.96^{b}	232.64 ± 6.95^{b}
Fx250	1.24±0.51^{b}	4.30 ±0.85^{b}	483.75± 22.31^{c}	636.31± 92.56^{b}	227.68± 6.29^{b}
Fx500	0.94±0.33^{b}	4.68±0.45^{b}	508.71±20.69^{c}	605.96± 155.14^{b}	276.00±13.10^{b}

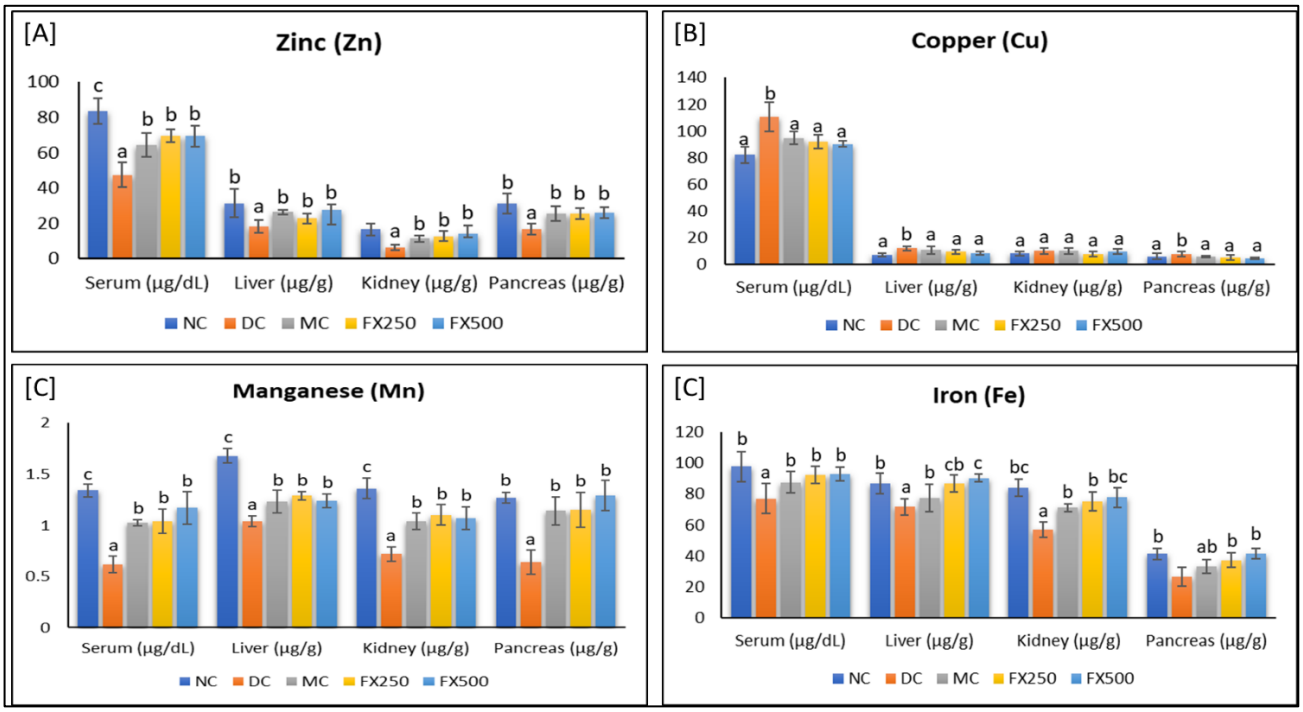

Figure 4: Effect of FX administration on antioxidant minerals levels in serum and tissues. [A]: Zinc (Zn); [B]: Copper (Cu);[C] Manganese (Mn); and [D]: Iron (Fe). Values are presented as mean ± SEM;n = 3. Experimental groups: NC (Normal Control); DC (Diabetic Control); MT (Metformin treated group); and FX_{250} and FX_{500} (formulation treated groups). Superscript letter ('a' 'b') indicates statistically significant differences between groups at P ≤ 0.05 level of significance.

3.2.5 Effect of FX administration on antioxidant enzyme activities

The results of the effect of FX administration on antioxidant enzyme activities in serum and organs (liver, kidney and pancreas) homogenates are presented in Table 1. The diabetic control group exhibited a significant ($P < 0.05$) increase in malondialdehyde (MDA) levels (5.77 ± 0.87 nmol/mL) and a significant ($P < 0.05$) decrease in glutathione (GSH) concentration (0.66 ± 0.06 µmol/L) in serum compared to the normal control group, which showed significantly ($P < 0.05$) lower MDA levels (1.61 ± 0.33 nmol/mL) and higher GSH concentrations (4.99 ± 0.54 µmol/L) (Table 1A). Furthermore, in the serum, the diabetic control group exhibited reduced activities of catalase (CAT), superoxide dismutase (SOD), and glutathione peroxidase (GPx) ($P < 0.05$) compared to the normal control (Table 1A). These observations indicate severe oxidative stress in the diabetic rats. Treatment with FX_{250} and FX_{500} for 3 weeks significantly reduced MDA levels ($P < 0.05$), bringing them closer to normal control values. Additionally, the activities of CAT, SOD, and GPx were significantly ($P < 0.05$) improved in the FX_{500}-treated group (305.38 ± 15.42 U/mL, 139.33 ± 4.7 U/mL, and 139.25 ± 7.5 U/mL), respectively compared to the diabetic untreated group (150.27 ± 13.47 U/mL, 60.85 ± 11.02 U/mL, and 85.58 ± 8.52 U/mL), respectively (Table 1A). Similar trends were observed in the liver, kidney, and pancreas tissues. These further reiterate the formulation's role in mitigating oxidative stress (Tables 1B, 1C, and 1D).

Table 1A, 1B, 1C and 1D: Effect of FX administration on antioxidant makers/enzyme activities. [1A]: Serum antioxidants [1B]: Liver antioxidants [1C]: Kidney antioxidants and [1D]: Pancreas antioxidants. Values are presented as mean ± SEM; n = 3. Experimental groups: NC (Normal Control), DC (Diabetic Control), MC (Metformin-treated group), and FX_{250} and FX_{500} (Formulation-treated groups). Superscript letter ('a' 'b' 'c') indicates statistically significant differences between groups at the P ≤ 0.05 level of significance.

3.2.6 Effect of FX administration on antioxidant minerals (Zn, Cu, Mn and Fe) concentrations

The results of the effect of FX administration on antioxidant minerals (Zn, Cu, Mn and Fe) concentrations

in the serum and tissue homogenates (liver, kidney and pancreas) of the alloxan induced diabetic rats are presented in Figure 4. The untreated diabetic group exhibited a significant ($P < 0.05$) decrease in Zn, Mn, and Fe concentrations in both serum and tissues compared to the normal control group (Figure 4A-4D). However, Cu levels were significantly elevated ($P < 0.05$) in the serum and liver of the diabetic untreated group compared with the normal control group (Figure 4B). These suggest alterations in antioxidant mineral homeostasis in the diabetic rats. However, treatment with the formulation (FX_{250} and FX_{500}) for three weeks resulted in the restoration/normalization of these minerals (Zn, Cu, Mn, and Fe) in both serum and tissues relative to the normal control group (Figure 4). These findings suggest that FX supplementation can replenish antioxidant minerals, mitigating oxidative stress-related mineral imbalances in diabetic conditions. Interestingly, observations similar to those in the FX_{500}-treated group were observed in the metformin-treated group (Figure 4D).

DISCUSSION OF THE RESULTS

4.1 In-vitro studies

Hyperglycemia-induced oxidative stress is a key factor in the pathogenesis of diabetes. Nutraceuticals with hypoglycemic and antioxidant properties offer a promising avenue for therapeutic potential, including in diabetes (Ghannadias and Lomer, 2022). *Abelmoschus esculentus* (okra) is known for its rich phytoconstituents, including phenols, flavonoids, fibers, and mucilage, with notable biological activities which contribute to its medicinal benefits (Durazzo et al., 2018). Previous studies highlight the antidiabetic properties of okra fruit, including the Ex-maradi variety, particularly its seeds and pods, leading to the formulation of an effective antidiabetic nutraceutical (Matazu et al., 2018; Muhammad et al., 2018; Abbas et al., 2017).

This study evaluated the antioxidant potential of the Ex-Maradi okra-based antidiabetic nutraceutical formulation in alloxan-induced diabetic rats. The formulation exhibited substantial total phenolic (61.84 ± 5.31 mg GAE/g) and total flavonoid (18.31 ± 2.17 mg QE/g) content, with strong *in-vitro* antioxidant activity, effectively scavenging hydrogen peroxide and superoxide radicals, and demonstrating relatively low IC_{50} values, providing direct free radical–scavenging capacity. This chemical antioxidant action likely contributes to an immediate reduction in oxidative stress following the administration. These findings align with previous reports on okra's antioxidant efficacy (Doreddula et al., 2014; Durazzo et al., 2018). The observed free radical-scavenging efficacy of FX may be attributed to the bioactive metabolites it produces, reinforcing its potential therapeutic role in managing oxidative stress.

The administration of alloxan (120 mg/kg) to the rats resulted in significantly elevated fasting blood glucose levels ($P < 0.05$) within 3 days. Clinical signs such as polyphagia, polydipsia, polyuria, and general stress manifestations confirmed the successful establishment of diabetes in the experimental rat model. The mechanism could involve selective beta-cell destruction by alloxan, via glucose transporter 2 (GLUT2), leading to the generation of reactive oxygen species (ROS), subsequent oxidative damages and impaired insulin secretion (Ajirioghene et al., 2021). This culminates in persistent hyperglycemia, contributing to the metabolic derangements characteristic of diabetes (Matazu et al., 2018). Three-week treatment with the formulation (FX_{250} and FX_{500}) significantly ($P < 0.05$) reduced blood glucose levels, comparable to metformin.

Additionally, the formulation modulated oxidative stress by improving antioxidant enzyme activities and normalizing the defective levels of antioxidant minerals. The hypoglycemic effect of the FX formulation may stem from its bioactive phytochemicals, which mitigate oxidative stress and thereby attenuate alloxan-induced oxidative injury to β-cells, enhancing pancreatic function and improving insulin sensitivity. These are supported from the medicinal benefit of *Abelmoschus esculentus* L. (okra) as previously reported by Mokgalaboni et al. (2024).

The exhibited significant ($P < 0.05$) weight loss in diabetic rats compared to normal control rats (Figure 3B) is likely due to impaired glucose metabolism and increased utilization of lipid and protein reserves (Ajirioghene et al., 2021). However, treatment with FX_{250} and FX_{500} led to weight restoration, suggesting improved insulin secretion and sensitivity, and a sustained glucose-lowering effect, thereby enhancing glucose uptake and utilization, suggesting the ability of FX to improve glucose metabolism and insulin sensitivity. These are consistent with previous findings on okra's role in metabolic syndromes (Nikpayam et al., 2024; Mokgalaboni et al., 2024), which support the antidiabetic potential of the FX formulation.

The organ index analysis revealed no significant ($P > 0.05$) differences in liver and kidney indices across all diabetic rats compared to the normal control rats (group), suggesting resilience of these organs to alloxan-induced oxidative stress. However, the significant reduction in pancreas index ($P < 0.05$) in diabetic rats highlights the pancreatic tissue's susceptibility to oxidative damage (Figure 3D). Treatment with the formulations significantly improved pancreatic indices, underscoring their protective effects on pancreatic integrity. This may also indicate the formulation's antioxidative effect, as generally supported by Doreddula et al. (2014). Nevertheless, more profound and biologically relevant effects were observed *in vivo,* where the treatment significantly improved endogenous antioxidant defences and glucose homeostasis.

The significant increase ($P < 0.05$) in malondialdehyde (MDA) levels in the serum and tissues, indicating heightened lipid peroxidation and oxidative stress, alongside reduced antioxidant enzyme activities (CAT, SOD, GPx) and glutathione (GSH) levels in serum and organ homogenates of the diabetic rats, indicate that the findings are consistent with the pro-oxidant nature of alloxan, which disrupts the antioxidant defence system via

ROS generation (Doma et al., 2023). Treatment with FX_{200} and FX_{500} significantly reduced lipid peroxidation and restored GSH levels, aligning with prior studies on antioxidant interventions of okra fruit (Doreddula et al., 2014). The observed protective effects are likely due to the formulation's phenolic flavonoids and other bioactive constituents, which scavenge ROS and mitigate oxidative damage. These may arise from suppression of gluconeogenesis through antioxidant-mediated signalling pathways. The concurrent reduction in MDA levels supports this interpretation, indicating that mitigation of oxidative damage plays a central role in restoring glucose metabolism (El Arem et al., 2014).

Furthermore, from the results, diabetes significantly ($P < 0.05$) reduced serum and organ levels of key antioxidant minerals, including zinc (Zn), copper (Cu), manganese (Mn), and iron (Fe), which serve as cofactors for critical antioxidant enzymes (SOD, GPx, and CAT). The depletion of these trace elements likely reflects their overutilization in counteracting oxidative stress (Dilworth et al., 2021; Uddin et al., 2021). Treatment with FX formulations restored mineral levels, supporting their role in enhancing antioxidant enzyme function and management of oxidative stress. The significant improvement in antioxidant enzyme activities (SOD, CAT, and GPx) observed in the treated diabetic rats, together with the concurrent elevation of essential antioxidant minerals (Zn, Cu, Mn, and Fe), suggests a synergistic mechanism through which the okra-based nutraceutical formulation exerts its antihyperglycemic and antioxidant effects. These findings align with prior research linking oxidative stress to trace mineral depletion and oxidative imbalance in diabetes (Pezonaga et al., 1996; Asadi et al., 2017; Ijarotimi et al., 2023). Many of these minerals act as obligatory cofactors in the catalytic machinery of endogenous antioxidant enzymes (Satyanarayana, 2021). For example, Cu and Zn are essential for the structural and catalytic integrity of Cu/Zn-SOD, while Mn serves as the central cofactor for mitochondrial Mn-SOD. Likewise, Fe is required for catalase activity, as its heme-dependent active site relies on Fe^{3+} for the dismutation of hydrogen peroxide (Satyanarayana, 2021; Liao et al., 2019). The improved mineral bioavailability could be attributed to the phytochemical composition of the formulation—particularly its phenolics and flavonoids—which are known to facilitate mineral absorption, stabilize metal ions, and modulate redox cycling (Satyanarayana, 2021). These may represent a key mechanistic dimension of the formulation's therapeutic effect.

CONCLUSION AND RECOMMENDATIONS

The okra-based nutraceutical formulation from ex-Maradi variety of *Abelmoscus esculentus* exhibited strong antioxidative and antidiabetic potential through multiple mechanisms. These findings support its use as a functional food or supplement for diabetes management, though more clinical trials are needed to provide definitive recommendations. Further research, including conducting a thorough chemical characterization of the FX formulation to identify the specific bioactive components responsible for its antioxidant and antidiabetic properties, and elucidating the precise mechanisms of action, is recommended. More pre-clinical and clinical trials are recommended to assess its clinical applicability and advance and commercialize innovations in diabetes management and other oxidative-related diseases.

AUTHOR CONTRIBUTIONS

Conceptualization and design of the work, Methodology, Statistical analysis: Muhammad I and Matazu K.I. Drafting of the manuscript: Muhammad I; Critical revision of the manuscript: Matazu K.I and Abbas A.Y. Laboratory works and handling of the animals: Aminu G.B, Musa T, Shamadeen AK and Muhammad I. All authors have reviewed the manuscript.

FUNDING

Thanks to the Tertiary Education Trust Fund (TETFund) Nigeria for funding this research through the Umaru Musa Yar'adua University Board of Research.

DATA AVAILABILITY

The datasets generated and/or analysed during the current study are available from the corresponding author upon reasonable request.

DECLARATIONS OF COMPETING INTERESTS

The authors declare no conflicts of interest.

REFERENCES

Abbas, A. Y., Muhammad, I., AbdulRahman, M. B., Bilbis, L. S., Saidu, Y., & Onu, A. (2017). Possible antidiabetic mechanism of action of ex-maradi okra fruit variety (Abelmoscus esculentus) on alloxan induced diabetic rats. *Nigerian Journal of Basic and Applied Sciences*, 25(2), 101–113. [Crossref]

Aebi, H. (1984). [13] Catalase in vitro. In *Methods in enzymology* (Vol. 105, pp. 121–126). Academic Press. [Crossref]

Ajirioghene, A. E., Ghasi, S. I., Ewhre, L. O., Adebayo, O. G., & Asiwe, J. N. (2021). Anti-diabetogenic and in vivo antioxidant activity of ethanol extract of *Dryopteris dilatata* in alloxan-induced male Wistar rats. *Biomarkers*, 26(8), 718–725. [Crossref]

Anjani, P., Damayanthi, E., , R., & Handharyani, E. (2018). Antidiabetic potential of purple okra (*Abelmoschus esculentus* L.) extract in streptozotocin-induced diabetic rats. *IOP Conference Series: Earth and Environmental Science*, 196. [Crossref]

Apak, R., Calokerinos, A., Gorinstein, S., Segundo, M. A., Hibbert, D. B., Gülçin, İ., Demirci Çekiç, S., Güçlü, K., Özyürek, M., & Çelik, S. E. (2022). Methods to evaluate the scavenging activity of antioxidants toward reactive oxygen and nitrogen

species (IUPAC Technical Report). *Pure and Applied Chemistry*, 94(1), 87–144. [Crossref]

Asadi, S., Moradi, M. N., Khyripour, N., Goodarzi, M. T., & Mahmoodi, M. (2017). Resveratrol attenuates copper and zinc homeostasis and ameliorates oxidative stress in type 2 diabetic rats. *Biological Trace Element Research*, 177, 132–138. [Crossref]

Athmuri, D. N., & Shiekh, P. A. (2023). Experimental diabetic animal models to study diabetes and diabetic complications. *MethodsX*, 11, 102474. [Crossref]

Bahari, H., Jazinaki, M., Rahnama, I., Aghakhani, L., Amini, M., & Malekahmadi, M. (2024). The cardiometabolic benefits of okra-based treatment in prediabetes and diabetes: A systematic review and meta-analysis of randomized controlled trials. *Frontiers in Nutrition*, 11. [Crossref]

Dilworth, L., Facey, A., & Omoruyi, F. (2021). Diabetes mellitus and its metabolic complications: The role of adipose tissues. *International Journal of Molecular Sciences*, 22(14), 7644. [Crossref]

Doma, A. O., Cristina, R. T., Dumitrescu, E., Degi, D., Moruzi, R. F., Brezovan, D., .. & Muselin, F. (2023). The antioxidant effect of *Aronia melanocarpa* extract in rats oxidative stress induced by cisplatin administration. *Journal of Trace Elements in Medicine and Biology*, 79, 127205. [Crossref]

Doreddula, S. K., Bonam, S. R., Gaddam, D. P., Desu, B. S. R., Ramarao, N., & Pandy, V. (2014). Phytochemical analysis, antioxidant, antistress, and nootropic activities of aqueous and methanolic seed extracts of ladies finger (*Abelmoschus esculentus* L.) in mice. *The Scientific World Journal*, 2014(1), 519848. [Crossref]

Durazzo, A., Lucarini, M., Novellino, E., Souto, E. B., Daliu, P., & Santini, A. (2018). *Abelmoschus esculentus* (L.): Bioactive components' beneficial properties—Focused on antidiabetic role—For sustainable health applications. *Molecules*, 24(1), 38. [Crossref]

El Arem, A., Zekri, M., Thouri, A., Saafi, E. B., Ghrairi, F., Ayed, A., ... & Achour, L. (2014). Oxidative damage and alterations in antioxidant enzyme activities in the kidneys of rat exposed to trichloroacetic acid: Protective role of date palm fruit. *Journal of Physiology and Biochemistry*, 70, 297–309. [Crossref]

Elkhalifa, A., Al-Shammari, E., Adnan, M., Alcantara, J., Mehmood, K., Eltoum, N., Awadelkareem, A., Khan, M., & Ashraf, S. (2021). Development and characterization of novel biopolymer derived from *Abelmoschus esculentus* L. extract and its antidiabetic potential. *Molecules*, 26. [Crossref]

Ellman, G. L., Courtney, K. D., Andres Jr, V., & Featherstone, R. M. (1961). A new and rapid colorimetric determination of acetylcholinesterase activity. *Biochemical Pharmacology*, 7(2), 88–95. [Crossref]

Ghannadias, F., & Lomer, B. B. (2022). Nutraceutical in the management of diabetes mellitus: A review. *Iranian Journal of Diabetes and Obesity*, 14(4), 240–247. [Crossref]

Gunas, V., Maievskyi, O., Raksha, N., Vovk, T., Savchuk, O., Shchypanskyi, S., & Gunas, I. (2023). Protein and peptide profiles of rats' organs in scorpion envenomation. *Toxicology Reports*, 10, 615–620. [Crossref]

Hamisu, S., & Salisu, B. (2025). GC-MS analysis and synergistic inhibition of *Staphylococcus aureus*, *Streptococcus pyogenes* and dermatophytes by novel plant oil blends developed for skin and hair therapy. *UMYU Journal of Microbiology Research (UJMR)*, 10(1), 284–295. [Crossref]

Ijarotimi, O., Akinola-Ige, A., & Oluwajuyitan, T. (2023). Okra seeds proteins: Amino acid profile, free radical scavenging activities and inhibition of diabetes and hypertensive converting enzymes indices. *Measurement: Food*. [Crossref]

Islam, M. M., Shova, N. A., Jahan, R., & Rahmatullah, M. (2022). Oral glucose tolerance test with methanol extract of leaves of *Ocimum minimum* L. (Lamiaceae) in Swiss albino mice. 10(5), 86–89. [Crossref]

Kharroubi, A. T., Darwish, H. M., Akkawi, M. A., Ashareef, A. A., Almasri, Z. A., Bader, K. A., & Khammash, U. M. (2015). Total antioxidant status in type 2 diabetic patients in Palestine. *Journal of Diabetes Research*, 2015(1), 461271. [Crossref]

Kizalaite, A., Brimiene, V., Brimas, G., Kiuberis, J., Tautkus, S., Zarkov, A., & Kareiva, A. (2019). Determination of trace elements in adipose tissue of obese people by microwave-assisted digestion and inductively coupled plasma optical emission spectrometry. *Biological Trace Element Research*, 189, 10–17. [Crossref]

Kottaisamy, C. P. D., Raj, D. S., Prasanth Kumar, V., & Sankaran, U. (2021). Experimental animal models for diabetes and its related complications—A review. *Laboratory Animal Research*, 37(1), 23, 1–14. [Crossref]

Lawrence, R. A., & Burk, R. F. (1976). Glutathione peroxidase activity in selenium-deficient rat liver. *Biochemical and Biophysical Research Communications*, 71(4), 952–958. [Crossref]

Liao, Z., Zhang, J., Liu, B., Yan, T., Xu, F., Xiao, F., Wu, B., Bi, K., & Jia, Y. (2019). Polysaccharide from Okra (*Abelmoschus esculentus* (L.) Moench) improves antioxidant capacity via PI3K/AKT pathways and Nrf2 translocation in a type 2 diabetes model. *Molecules*, 24. [Crossref]

Marklund, S., & Marklund, G. (1974). Involvement of the superoxide anion radical in the autoxidation of pyrogallol and a convenient assay for superoxide dismutase. *European Journal of Biochemistry*, 47(3), 469–474. [Crossref]

Matazu, K. I., Ismaila, M., Bilbis, L., & Abbas, A. Y. (2018). Formulation of okra-based antidiabetic nutraceutical from *Abelmoschus esculentus* (L.) Moench (Ex-maradi variety) and evaluation of its effect on alloxan-induced diabetic rats.

International Journal of Current Research and Review, 10, 11–16. [Crossref]

Mokgalaboni, K., Lebelo, S., Modjadji, P., & Ghaffary, S. (2023). Okra ameliorates hyperglycaemia in pre-diabetic and type 2 diabetic patients: A systematic review and meta-analysis of the clinical evidence. *Frontiers in Pharmacology*, 14. [Crossref]

Mokgalaboni, K., Phoswa, W. N., Mokgalabone, T. T., Dlamini, S., Ndhlala, A. R., Modjadji, P., & Lebelo, S. L. (2024). Effect of *Abelmoschus esculentus* L. (okra) on dyslipidemia: Systematic review and Meta-analysis of clinical studies. *International Journal of Molecular Sciences*, 25(20), 10922. [Crossref]

Muhammad, I., Matazu, I. K., Yaradua, I. A., Yau, S., Nasir, A., Bilbis, S. L., & Abbas, Y. A. (2018). Development of okra-based antidiabetic nutraceutical formulation from *Abelmoschus esculentus* (L.) Moench (Ex-maradi variety). *Tropical Journal of Natural Product Research*, 2(2), 80–86. [Crossref]

Nasrollahi, Z., Shahanipour, K., Monajemi, R., & Ahadi, A. (2022). *Abelmoschus esculentus* (L.) Moench improved blood glucose, lipid, and down-regulated PPAR-α, PTP1B genes expression in diabetic rats. *Journal of Food Biochemistry*, e14097. [Crossref]

Nikpayam, O., Safaei, E., Bahreini, N., & Saghafi-Asl, M. (2021). The effects of okra (*Abelmoschus esculentus* L.) products on glycemic control and lipid profile: A comprehensive systematic review. *Journal of Functional Foods*. [Crossref]

Nikpayam, O., Saghafi-Asl, M., Safaei, E., Bahreyni, N., Sadra, V., & Asgharian, P. (2024). The effect of *Abelmoschus esculentus* L. (Okra) extract supplementation on glycaemic control, inflammation, kidney function and expression of PPAR-α, PPAR-γ, TGF-β and Nrf-2 genes in patients with diabetic nephropathy: A triple-blind, randomized, placebo-controlled trial. *British Journal of Nutrition*, 131(4), 648–657. [Crossref]

Ohkawa, H., Ohishi, N., & Yagi, K. (1979). Assay for lipid peroxides in animal tissues by thiobarbituric acid reaction. *Analytical Biochemistry*, 95(2), 351–358. [Crossref]

Patwardhan, J., & Bhatt, P. (2016). Flavonoids derived from *Abelmoschus esculentus* attenuates UV-B induced cell damage in human dermal fibroblasts through Nrf2-ARE pathway. *Pharmacognosy Magazine*, 12(Suppl 2), S129–S138. [Crossref]

Pezonaga, A., Taylor, M., & Dobrota, D. (1996). The effects of platinum chemotherapy on essential trace elements. *European Journal of Cancer Care*, 5(2), 122–126. [Crossref]

Phoswa, W. N., & Mokgalaboni, K. (2023). Comprehensive overview of the effects of *Amaranthus* and *Abelmoschus esculentus* on markers of oxidative stress in diabetes mellitus. *Life*, 13(9), 1830. [Crossref]

Phuyal, N., Jha, P. K., Raturi, P. P., & Rajbhandary, S. (2020). Total phenolic, flavonoid contents, and antioxidant activities of fruit, seed, and bark extracts of *Zanthoxylum armatum* DC. *The Scientific World Journal*, 2020(1), 8780704. [Crossref]

Roy, A., Shrivastava, S. L., & Mandal, S. M. (2014). Functional properties of Okra *Abelmoschus esculentus* L. (Moench): Traditional claims and scientific evidences. *Plant Science Today*, 1(3), 121–130. [Crossref]

Salisu, B., Anua, M. S., Wan Ishak, W. R., & Mazlan, N. (2020). Incidence, distribution and phenotypic characterisation of aflatoxigenic fungi contaminating commonly consumed food grains in Katsina State, Nigeria. *Malaysian Journal of Medicine and Health Sciences*, 16(SUPP11), 2636–9346.

Salisu, Dandashire, B., Magashi, A. M., Abdulkadir, B., Abbas, M. A., Dauda Goni, M., & Yakubu, A. (2019). Toxicological studies and bioactivity-guided identification of antimicrobially active compounds from crude aqueous stem bark extract of *Boswellia dalzielii*. *Journal of Advanced Veterinary and Animal Research*, 6(2), 183–192. [Crossref]

Satyanarayana, U. (2021). Biochemistry 6e-E-book. Elsevier Health Sciences.

Sereno, A. B., Pinto, C. D., Andrade, F. A., da Silva, M. A. B., Garcia, A. C., Krüger, C. C. H., & de Messias Reason, I. J. (2022). Effects of okra (*Abelmoschus esculentus* (L.) Moench) on glycemic markers in animal models of diabetes: A systematic review. *Journal of Ethnopharmacology*, 298, 115544. [Crossref]

Sharifi-Rad, M., Anil Kumar, N. V., Zucca, P., Varoni, E. M., Dini, L., Panzarini, E., Rajkovic, J., Tsouh Fokou, P. V., Azzini, E., & Peluso, I. (2020). Lifestyle, oxidative stress, and antioxidants: Back and forth in the pathophysiology of chronic diseases. *Frontiers in Physiology*, 11, 694. [Crossref]

Sun, X., Wang, M., Xu, C., Wang, S., Li, L., Zou, S., ... & Wei, Y. (2022). Positive effect of a pea-clam two-peptide composite on hypertension and organ protection in spontaneously hypertensive rats. *Nutrients*, 14(19), 4069. [Crossref]

Tavakolizadeh, M., Peyrovi, S., Ghasemi-Moghaddam, H., Bahadori, A., Mohkami, Z., Sotoudeh, M., & Ziaee, M. (2023). Clinical efficacy and safety of okra (*Abelmoschus esculentus* (L.) Moench) in type 2 diabetic patients: A randomized, double-blind, placebo-controlled, clinical trial. *Acta Diabetologica*, 60(12), 1685–1695. [Crossref]

Tesauro, M., & Mazzotta, F. A. (2020). Pathophysiology of diabetes. In *Transplantation, bioengineering, and regeneration of the endocrine pancreas* (pp. 37–47). Academic Press. [Crossref]

Uddin Zim, A. F. M. I., Khatun, J., Khan, M. F., Hossain, M. A., & Haque, M. M. (2021). Evaluation of in vitro antioxidant activity of okra mucilage and its antidiabetic and antihyperlipidemic effect in alloxan-induced diabetic mice. *Food Science and Nutrition*, 9(12), 6854–6865. [Crossref]

Usman, Z., Fatima, M., Salisu, B., & Dandashire, A. S. (2025). Integrated phytochemical profiling (GC-

MS/FTIR), molecular docking, and bioevaluation of *Vernonia amygdalina* and *Psidium guajava* against multidrug- resistant *Salmonella typh*. *UMYU Scientifica*, 4(4), 88–111. [Crossref]

Woumbo, C., Kuate, D., Tamo, D., & Womeni, H. (2022). Antioxidant and antidiabetic activities of a polyphenol rich extract obtained from *Abelmoschus esculentus* (okra) seeds using optimized conditions in microwave-assisted extraction (MAE). *Frontiers in Nutrition*, 9. [Crossref]

Yasin, H., Tariq, F., Sameen, A., Ahmad, N., Manzoor, M. F., Yasin, M., Tariq, T., Iqbal, M. W., Ishfaq, B., & Mahmood, S. (2020). Ethanolic extract of okra has a potential gastroprotective effect on acute gastric lesions in Sprague Dawley rats. *Food Science & Nutrition*, 8(12), 6691–6698. [Crossref]

Yusof, A. F. M. (2020). Best practice for the care and use of animals in experimentation: A Malaysian perspective. *Ulum Islamiyyah*, 30, 13–26. [Crossref]